

Decomposition of Dichlorodifluoromethane with Simultaneous Halogen Fixation by Vanadium Oxide Supported on Magnesium Oxide

Tsukasa Tamai, Koji Inazu, and Ken-ichi Aika*

Department of Environmental Chemistry and Engineering, Interdisciplinary Graduate School of Science and Engineering, Tokyo Institute of Technology, 4259-G1-13 Nagatsuta, Midori-ku, Yokohama 226-8502

Received February 8, 2005; E-mail: kenaika@chemenv.titech.ac.jp

Dichlorodifluoromethane (CCl_2F_2, 1% in He) decomposition with simultaneous halogen fixation by vanadium oxide supported on magnesium oxide was studied at 723 K in a flow apparatus. The pretreatment condition and vanadium loading of supported vanadium oxide samples affected the CCl_2F_2 decomposition efficiency. Through characterization studies (XRD, IR, Raman, and XPS) and reference experiments, $Mg_3(VO_4)_2$ was revealed to be the active species to initiate CCl_2F_2 decomposition, leading to MgF_2, $MgCl_2$, and CO_2 formation. The model experiments also suggested a detailed mechanism that $VOCl_3$ was formed from $Mg_3(VO_4)_2$ by a reaction with CCl_2F_2 or the major intermediate compound CCl_4, and that $VOCl_3$ reacted with MgO to regenerate $Mg_3(VO_4)_2$ and to promote chlorine fixation as $MgCl_2$.

Since chlorofluorocarbons (CFCs) are believed to be a major source of depletion of the stratospheric ozone layer, CFCs are totally phased out now. However, there is a large amount of CFCs remaining in refrigerators and air-conditioners, which should be decomposed to be harmless to the environment. Direct mineralization of such harmful halocarbons to metal halides and CO_2 is a desirable method to decompose them without the formation of corrosive HCl and HF. Klabunde et al. have found that nano-crystalline MgO and CaO are effective for the destructive absorbent of some hazardous compounds, like CCl_4.[1–6] They found that the addition of a small amount of transition metal oxide promoted the reaction with CCl_4 to almost stoichiometric decomposition under a certain condition.[1,2] The role of such transition metal oxides has been reported to promote O^{2-}–Cl^- exchange in the solid phase;[2,3] e.g. MOx/MgO reacts with CCl_4 to form $MCly$/MgO, and then the solid state oxygen–halogen exchange reaction occurs to regenerate MOx ($MOx/MgCl_2$), where x and y are the numbers of oxygen and chlorine that are specific for the kind of metal. We have reported an application of this method to the decomposition of CCl_2F_2 using MgO as an absorbent.[7,8] In our previous work, it was found that while the addition of transition metal oxide to MgO enhanced the conversion of CCl_2F_2, the selective decomposition to CO_2 with halogen fixation as MgF_2 and $MgCl_2$ sufficiently proceeded only with vanadium oxide supported on MgO following;

$$CCl_2F_2(g) + 2MgO(s) \rightarrow CO_2(g) + MgCl_2(s) + MgF_2(s) \quad \Delta H^0 = -477\ \mathrm{kJ\,mol^{-1}}. \quad (1)$$

Oxides of Mn, Fe, Co, and Cu supported on MgO showed CO_2 selectivity of 50% and yielded an equimolar amount of CCl_4, and only fluorine fixation as MgF_2 occurred, although maximum CCl_2F_2 conversion reached 100% at 723 K. In this case, the reaction equation is described as

$$2CCl_2F_2(g) + 2MgO(s) \rightarrow CO_2(g) + CCl_4(g) + 2MgF_2(s) \quad \Delta H^0 = -578\ \mathrm{kJ\,mol^{-1}}. \quad (2)$$

We studied the role of the fluorination of MgO in the reaction mechanism of CCl_2F_2 decomposition. Partial fluorination of MgO provides strong Lewis acidity to MgO and promotes CCl_2F_2 conversion to CCl_4,[8] though oxides of Mn, Fe, Co, and Cu supported on MgO have the same role. Once partially fluorinated MgO is formed during the decomposition of CCl_2F_2, the reaction proceeds autocatalytically. On the other hand, vanadium oxide supported on MgO is the only effective sample to show the decomposition of CCl_2F_2 to CO_2. Although vanadium oxide is considered to work as a catalyst for the conversion of CCl_2F_2 to CO_2 and magnesium halides, the mechanism has not been well understood. In the present work, we investigated the catalytic role of vanadium oxide by focusing on the transformation of vanadium species to affect chlorine fixation in CCl_2F_2 decomposition.

Results and Discussion

CCl_2F_2 Decomposition Reactivity of Vanadium Oxide Supported on Magnesium Oxide. CCl_2F_2 decomposition was carried out using vanadium oxide supported on MgO samples treated under air (VM-air) or helium (VM-He) with different vanadium loading. The time course of CCl_2F_2 conversion at 723 K is shown in Fig. 1. At this temperature MgO showed no reactivity to CCl_2F_2, although it can react with CCl_2F_2 significantly at temperature higher than 873 K.[8] For CCl_2F_2 decomposition with a 1 wt% vanadium loaded sample (1VM-air), a short induction period was observed before reaching CCl_2F_2 conversion of 100%, while for 5VM-air and 30VM-air 100% conversion started from the beginning of the reaction. For VM-He samples, no induction period was observed, even for a 1 wt% vanadium loaded sample.

The cumulative conversions of CCl_2F_2 and MgO, CO_2 selectivity, and CO selectivity after the reaction for 3 h, when CCl_2F_2 loading reached nearly a stoichiometric amount to MgO (0.45 $\mathrm{mol\,mol^{-1}}$), are listed in Table 1 together with the BET surface area of the samples. The cumulative MgO conversion was calculated based on the amount of oxygen

Published on the web August 4, 2005; DOI 10.1246/bcsj.78.1565

atom in CO and CO_2 formed by the reaction, assuming that all of the samples had MgO of 0.2 g (5.0 mmol).

The formation of CO was observed for helium-treated samples, and the amount of CO increased as vanadium loading increased. On the other hand, CO was not formed at all with any VM-air samples used, and the CO_2 selectivity was quite high as 96% for 5VM-air. For 1VM-air the CO_2 selectivity was slightly lower than that for 5VM-air, and the formation of a small amount of CCl_4 was observed. High CO_2 selectivity resulted in a high conversion of MgO, meaning high halogen-absorption ability. 5VM-air showed the highest MgO conversion of 75% to be the most preferable sample for halogen fixation among the samples used.

Figure 2 shows CO_2 yield as a function of the MgO conversion for 1VM-air and 5VM-air samples. As long as MgO conversion is below 40%, a high CO_2 yield is maintained, while the CO_2 yield gradually decreased after MgO conversion passes over 60%. In short, the reactivity depends on the amount of remaining MgO, but not on vanadium loading if some amount of vanadium is loaded. These results indicate that the decomposition proceeds catalytically over the vanadium species, and that the yield of CO_2 depends strongly on the available amount of MgO.

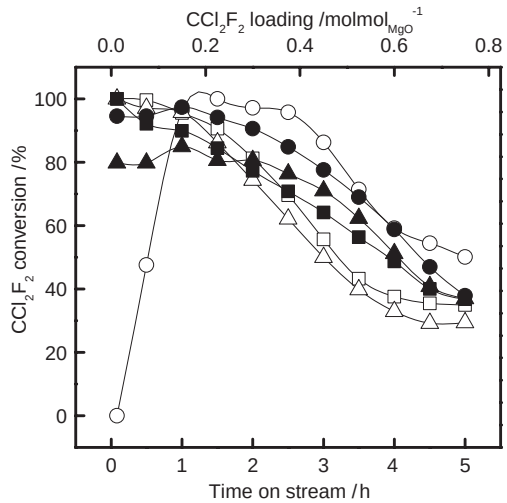

Fig. 1. CCl_2F_2 decomposition by VM-air (open) and VM-He (closed) sample. Vanadium loading: 1 wt% (○, ●), 5 wt% (□, ■), and 30 wt% (△, ▲). Reaction temperature: 723 K, reaction gas: 1% CCl_2F_2 (diluted with helium), 30 mL min^{-1}.

The time course of the reaction by 5VM-air is shown in Fig. 3. Both the initial CCl_2F_2 conversion and the CO_2 selectivity are almost 100%, indicating that 100% of CCl_2F_2 is decomposed to $MgCl_2$ and MgF_2 exclusively (Eq. 1). However, the CCl_2F_2 conversion and the CO_2 selectivity decrease with time i.e. with an increase in the MgO conversion, where CCl_4 is started to form, and becoming the major product at last. CCl_4 can be formed through either as Eq. 2 or

$$CCl_2F_2(g) + MgCl_2(s) \rightarrow CCl_4(g) + MgF_2(s), \quad \Delta H^0 = -100\ \text{kJ mol}^{-1}. \tag{3}$$

The same amount of CO_2 and CCl_4 should be formed according to Eq. 2. If formed CCl_4 was decomposed by the following reaction, the CO_2 selectivity should exceed 50%. This suggests that the fixation of formed CCl_4 is a key process for complete halogen fixation as MgF_2 and $MgCl_2$:

$$CCl_4(g) + 2MgO(s) \rightarrow CO_2(g) + 2MgCl_2(s), \quad \Delta H^0 = -376\ \text{kJ mol}^{-1}. \tag{4}$$

After 4 h of the reaction, MgO conversion reaches about 80% with a high CCl_4 selectivity of 50%. The CCl_4 selectivity finally reaches over 70% after 5 h of the reaction. This high CCl_4 selectivity cannot be explained without assuming Eq. 3. In short, CCl_2F_2 can react with both MgO and $MgCl_2$; when MgO conversion exceeds 80%, the reaction with $MgCl_2$ be-

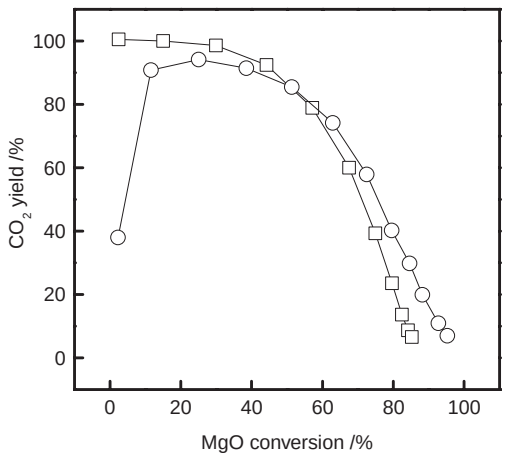

Fig. 2. CO_2 yield as a function of MgO conversion. Vanadium loading: 1 wt% (○) and 5 wt% (□). Reaction temperature: 723 K, reaction gas: 1% CCl_2F_2 (diluted with helium), 30 mL min^{-1}.

Table 1. The Results of CCl_2F_2 Decomposition for Various Vanadium Oxide Loaded MgO

Sample	Surface area /$m^2\ g^{-1}$	CCl_2F_2 conv.[a] /%	MgO conv.[b] /%	CO_2 select. /%	CO select. /%
1VM-He	147	91	64	81	6
5VM-He	120	82	68	91	9
30VM-He	161	80	68	85	18
1VM-air	120	84	68	91	0
5VM-air	139	86	75	96	0
30VM-air	48	82	69	94	0

Reaction temperature: 723 K, reaction gas: CCl_2F_2 1% (diluted by helium), 30 mL/min. Reaction time: 3 h, weight of vanadium oxide loaded MgO: 0.2 g. a) Cumulative conversion. b) MgO conversion based on the total amount of oxygen in formed CO_2 and CO throughout the reaction.

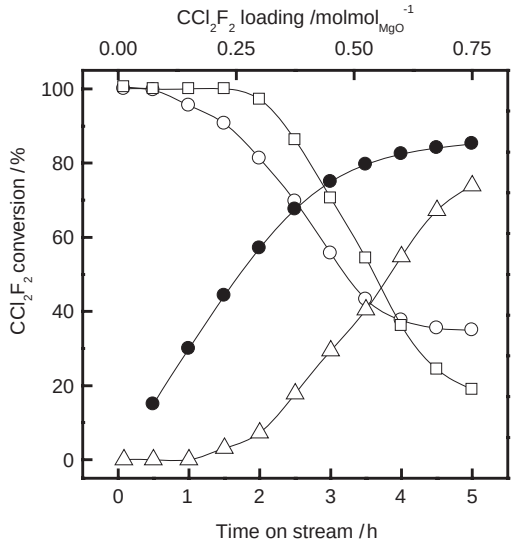

Fig. 3. Time course of CCl_2F_2 decomposition by 5VM-air. CCl_2F_2 conversion (○), MgO conversion (●), CO_2 selectivity (□), and CCl_4 selectivity (△). Reaction temperature: 723 K, reaction gas: 1% CCl_2F_2 (diluted with helium), 30 mL min^{-1}.

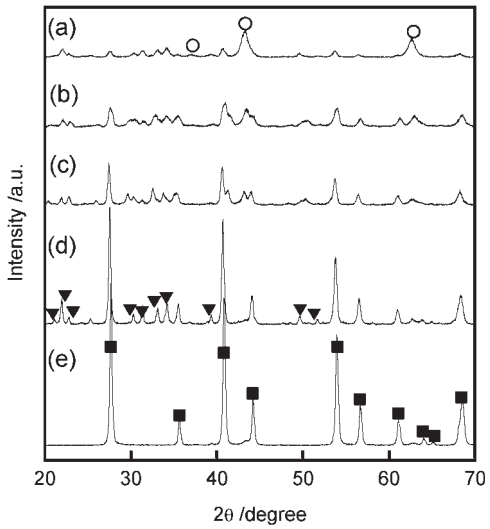

Fig. 4. XRD patterns of 5VM-air sample after the reaction with CCl_2F_2 for (a) 1 h, (b) 3 h, (c) 5 h, (d) 10 h, and (e) 25 h. Reaction temperature: 723 K, amount of 5VM-air sample: 0.2 g. MgO (○), MgF_2 (■), and $MgCl_2 \cdot 6H_2O$ (▼).

comes the main reaction due to the low concentration of MgO. Of course, the $MgCl_2$ conversion reaction (Eq. 3) is slower than Eq. 2 at the beginning of the reaction.

Some authors have reported the halogen exchange or disproportionation of CCl_2F_2 to CCl_3F and $CClF_3$ on alumina-based catalysts.[9,10] In these reactions, disproportionation of formed CCl_3F to CCl_4 and CCl_2F_2 also occurs sequentially. By 5 h of the reaction studied here, a trace amount of CCl_3F was observed, while no $CClF_3$ was detected. This fact shows that the disproportionation reaction does not occur in this system under the employed condition.

XRD patterns of the 5VM-air sample after the reaction for different periods of time are shown in Fig. 4. After the reaction for 10 h, or shorter, patterns originating from both MgF_2 and $MgCl_2$ were observed. $MgCl_2$ was observed as hexahydrate, the most stable $MgCl_2$ hydrate, because $MgCl_2$ is highly hygroscopic to have water absorbed during the handling of the samples after the reaction. As the reaction prolonged, the peaks due to MgF_2 became intense and those from MgO became small. Finally, for a reaction of 25 h, the XRD pattern was completely changed to that of MgF_2, and the peaks from $MgCl_2$ and MgO were completely disappeared. The result agrees with the products changed during the reaction shown in Fig. 3. In the following part, we focus mainly on the state of air-treated vanadium oxide supported on a MgO sample (VM-air) to clarify the detailed mechanism.

Characterization of VM Sample. Among the oxide supports, MgO has unique characteristics in supporting vanadium oxide. For its basic character, the interaction with V_2O_5 is strong, and hence composite oxide phases of vanadium and magnesium are formed.[11,12] The chemical forms of the composite oxides depend on the ratio of vanadium to magnesium and on the preparation condition, such as the calcination temperature or time.[11,13] So far, MgV_2O_6, $Mg_2V_2O_7$, and $Mg_3(VO_4)_2$ are known as the magnesium vanadate. These compounds have

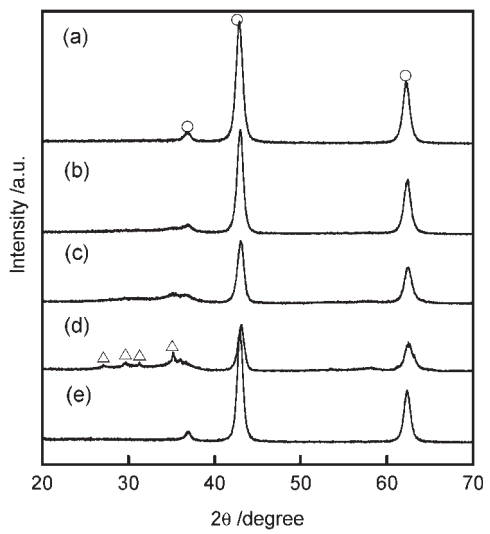

Fig. 5. XRD patterns of vanadium oxide loaded MgO. (a) 5VM-air, (b) 10VM-air, (c) 20VM-air, (d) 30VM-air, and (e) 30VM-He. MgO (○) and $Mg_3(VO_4)_2$ (△).

been investigated mainly as the catalyst for the oxidative dehydrogenation of light alkanes.[11–19,22,23]

While 5VM-air showed only peaks of MgO in its XRD pattern (Fig. 5a), the $Mg_3(VO_4)_2$ phase was slightly observed for 10% VM-air (Fig. 5b). As vanadium loading increased, the diffraction pattern of $Mg_3(VO_4)_2$ was clearly observed. Only the diffraction pattern of MgO was observed for VM-He samples, even when vanadium loading was 30 wt % (Fig. 5e). There have been many reports showing that vanadium-containing phases can be observed in the MgO matrix only for samples with high vanadium loading.

The FT-IR spectra of reference vanadium compounds and VM samples are shown in Fig. 6. A characteristic peak of V=O bonding was observed at a wavenumber of 1022 cm^{-1} for V_2O_5, and two characteristic peaks of isolated VO_4 tetrahe-

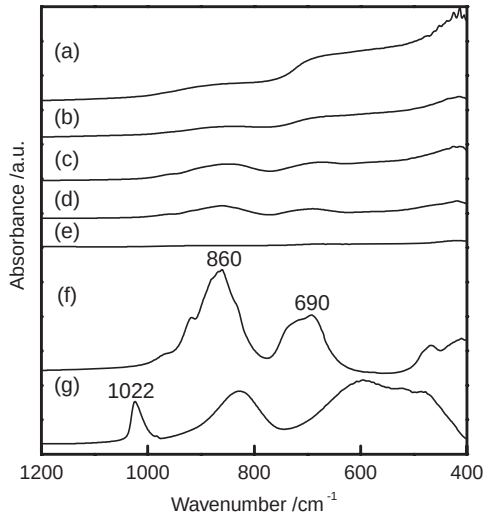

Fig. 6. IR spectra of VM samples and authentic vanadium oxides. (a) 5VM-air, (b) 10VM-air, (c) 20VM-air, (d) 30VM-air, (e) 30VM-He, (f) $Mg_3(VO_4)_2$, and (g) V_2O_5.

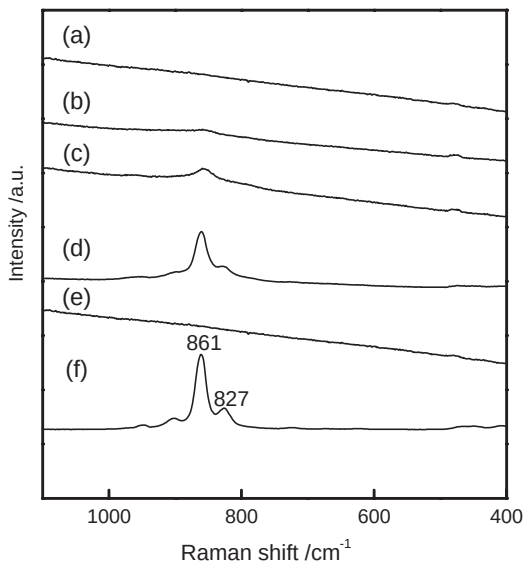

Fig. 7. Raman spectra of VM samples and $Mg_3(VO_4)_2$. (a) 5VM-air, (b) 10VM-air, (c) 20VM-air, (d) 30VM-air, (e) 30VM-He, and (f) $Mg_3(VO_4)_2$.

dron and V–O–V bond were observed at 860 cm^{-1} and 690 cm^{-1} for $Mg_3(VO_4)_2$.[13] The spectrum for $Mg_3(VO_4)_2$ was consistent with the reported ones.[13,14]

Two peaks at 860 cm^{-1} and 690 cm^{-1} were observed for VM-air at vanadium loading of 20% and 30% as the same as $Mg_3(VO_4)_2$, and increased in intensity as vanadium loading increased. No characteristic peak of V=O bond of V_2O_5 was observed for any VM-air samples. For VM-He samples, even at vanadium loading of 30 wt %, there was no distinct peak, indicating a vanadium-containing phase.

The Raman spectra for VM samples and $Mg_3(VO_4)_2$ are also shown in Fig. 7. $Mg_3(VO_4)_2$ has characteristic peaks at Raman shifts of 861 cm^{-1} and 827 cm^{-1}.[14,18,19] For 20VM-air, a distinct peak at 861 cm^{-1}, which is a characteristic peak of $Mg_3(VO_4)_2$, was observed. At higher vanadium loading of 30 wt %, peaks at 861 cm^{-1} and 827 cm^{-1} became strong, while VM-He showed no peak in this range, even at the same vanadium loading. VM-He samples had two peaks at 1350 cm^{-1} and 1600 cm^{-1} due to the deposition of elemental carbon on the MgO surface during the decomposition of the precursor acetylacetonate complex in the sample preparation, while such carbon-derived peaks were not observed for VM-air samples, since elemental carbon could be easily removed by calcination under air. This difference concerning the existence of a carbonaceous species on the MgO surface could influence the ability of CCl_2F_2 decomposition, but the influence is not clear at this point.

XRD, FT-IR, and Raman analyses gave consistent results. VM-air samples were found to contain $Mg_3(VO_4)_2$, and its content increased with an increase in vanadium loading. On the other hand, evidence neither for the formation of magnesium vanadate nor of vanadium oxides was observed, even at vanadium loading of 30 wt % for VM-He samples. Vanadium acetylacetonate, which was used as a precursor of vanadium oxide in the sample preparation, changed into not only V_2O_5, but also V_2O_3 by thermal decomposition under an inert atmosphere (e.g. nitrogen), since CO formed from the ligand in the decomposition could reduce, at least, part of V_2O_5 to V_2O_3.[20] A smaller amount of V_2O_5 formed in the case of VM-He samples may have suppressed the formation of $Mg_3(VO_4)_2$.

The crystal structure of $Mg_3(VO_4)_2$ has been reported by Krishnamachari and Calvo.[21] It consists of nearly cubic closest packing of oxygen atom layers with the Mg ions in octahedral sites and the V ions in tetrahedral sites.

NH_3-TPD. In our previous report the acid character of MgO has been pointed out to be an important factor concerning CCl_2F_2 decomposition. Thus, NH_3-TPD was carried out to determine the amount of acid on VM-air samples. The results are shown in Fig. 8 and listed in Table 2 for five kinds of VM-air, MgO, and $Mg_3(VO_4)_2$ samples. As vanadium loading was increased, the acid strength and the acid amount drastically in-

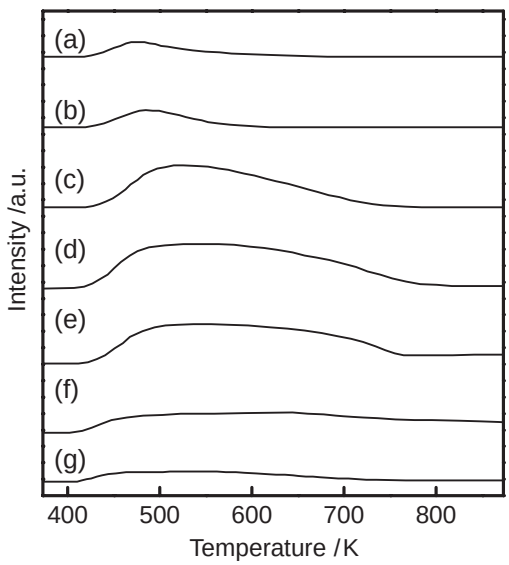

Fig. 8. NH_3-TPD profiles of MgO, VM samples, and $Mg_3(VO_4)_2$. (a) MgO, (b) 1VM, (c) 3VM, (d) 5VM, (e) 10VM, (f) 30VM, and (g) $Mg_3(VO_4)_2$.

creased, and became the maximum at 180 μmol g^{-1} for 5VM-air or 10VM-air and then decreased when vanadium loading reached 30 wt %. On the other hand, a specific amount of adsorbed NH_3 against the surface area of the sample increased as vanadium loading was increased; the $Mg_3(VO_4)_2$ sample had the highest value (4.98 μmol m^{-2}). It has been reported that V–Mg–O catalysts containing $Mg_3(VO_4)_2$ bear Lewis acidity and no Brønsted acidity.[12,22,23] Thus, the generation of acid sites on VM-air samples should be related to the formation of $Mg_3(VO_4)_2$.

XPS. XPS spectra were taken for MgO, $Mg_3(VO_4)_2$, and two kinds of VM-air samples. Each binding energy of O1s, Mg2p, and $V2p_{3/2}$ peaks and atomic ratio of V to Mg are shown in Table 3. The V/Mg ratio at the surface was almost the same as that of the bulk for the 5VM-air sample. For the 30VM-air sample, the surface V/Mg ratio of 0.47 was higher than that of the bulk (0.24), and rather similar to that of $Mg_3(VO_4)_2$ (0.62). The binding energies of O1s, Mg2p, and $V2p_{3/2}$ were almost the same for all of the vanadium containing samples. The binding energy of Mg2p of MgO was 49.0 eV, which is about 0.5 to 1.0 eV lower than those of the other samples. This fact indicates that Mg becomes more cationic[24] by supporting vanadium oxide, even at vanadium loading of 5 wt %, and that the Mg cation can be the Lewis acidic center, which is effective to dissociate C–F bonding.

CCl_2F_2 Decomposition by Vanadium Oxides and Magnesium Vanadates. The reactivity of vanadium oxides and magnesium vanadates to CCl_2F_2 were studied and compared to those of VM samples. The results of CCl_2F_2 decomposition by them for 3 h are listed in Table 4 along with the BET surface area of the sample. V_2O_5 and V_2O_4 did not react with CCl_2F_2, while V_2O_3 showed appreciable reactivity to CCl_2F_2. This result suggests that the oxidation state of vanadium influences the reactivity to CCl_2F_2 and that V_2O_3 is an active phase.

Only $Mg_3(VO_4)_2$ was able to decompose CCl_2F_2 significantly among three kinds of magnesium vanadates. Although the difference in the reactivity should be partly due to the difference in the surface area, it is clear that $Mg_3(VO_4)_2$ is an active phase for CCl_2F_2 decomposition. A remarkable result was that CO_2 was the only gas-phase product in CCl_2F_2 decomposition by $Mg_3(VO_4)_2$, indicating the CO_2 selectivity was 100%. In this reaction, a dark yellowish-red cloud of vapor was observed at the outlet of the reactor, indicating the formation of $VOCl_3$.[25] $VOCl_3$ is a pale-yellow liquid at room temperature, and its melting point and boiling point are 194 K and 400 K, respectively. The reddish cloud of vapor gradually changed into an orange-colored deposit, and the color finally changed to dark green. The role of $VOCl_3$ in CCl_2F_2 decomposition is mentioned in the following discussion. Moreover, a yellowish deposit was also observed at the upper port of the reactor. Judging from the color, it should be VOF_3 or V_2O_5.[26] The melting point and boiling point of VOF_3 are 573 K and 753 K, respectively. At a reaction temperature of 723 K, VOF_3 must be in the liquid phase.

Table 2. Specific Surface Area and NH_3-TPD Results for VM-air Samples, MgO, and $Mg_3(VO_4)_2$

Sample	Surface area /m^2 g^{-1}	Adsorbed NH_3	
		μmol g^{-1}	μmol m^{-2}
MgO	192	18	0.09
1VM	132	23	0.17
3VM	152	125	0.83
5VM	139	182	1.31
10VM	111	179	1.61
30VM	48	126	2.62
$Mg_3(VO_4)_2$	16	80	4.98

Table 3. Results of XPS Analysis for VM-air Samples, MgO, and $Mg_3(VO_4)_2$

Sample	Binding energy/eV			Atomic ratio	
	O1s	$V2p_{3/2}$	Mg2p	V/M[a)]	V/Mg (bulk)[b)]
MgO	529.3	—	49.0	—	—
5VM-air	529.5	517.0	49.5	0.06	0.04
30VM-air	530.0	517.0	49.8	0.47	0.24
$Mg_3(VO_4)_2$	530.1	517.4	50.0	0.64	0.67

a) Estimated by XPS peak area of $V2p_{3/2}$ and Mg2p. b) Bulk ratio assuming that vanadium loss was not observed during sample preparation.

Table 4. Specific Surface Area and the Results of CCl_2F_2 Decomposition for Authentic Vanadium Oxides and Magnesium Vanadates

Sample	Surface area /m^2 g^{-1}	CCl_2F_2 conv.[a)] /%	Metal oxide conv.[b)] /%	CO_2 select. /%	CO select. /%
V_2O_3	2.6	62	15	32	4
V_2O_4	0.8	0	0	0	0
V_2O_5	7.2	0	0	0	0
$Mg_3(VO_4)_2$	14.3	63	35	100	0
MgV_2O_6	2.2	0	0	0	0
$Mg_2V_2O_7$	5.4	0	0	0	0

Reaction temperature: 723 K, reaction gas: CCl_2F_2 1% (diluted with helium), 30 mL/min. Reaction time: 3 h, weight of sample: 0.2 g. a) Maximum conversion obtained during the reaction. b) Estimated using total amount of oxygen evolved as CO_2 and CO.

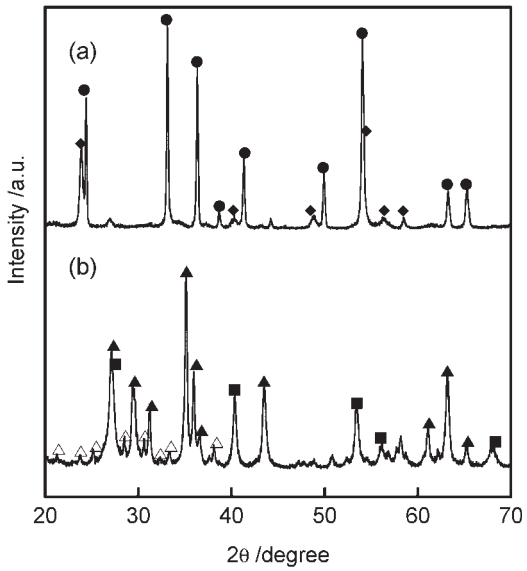

Fig. 9. XRD patterns of (a) V_2O_3 and (b) $Mg_3(VO_4)_2$ after the reaction with CCl_2F_2 at 723 K for 5 h. V_2O_3 (●), VF_3 (◆), $Mg_3(VO_4)_2$ (▲), MgF_2 (■), and $Mg_2V_2O_7$ (△).

XRD patterns of V_2O_3 and $Mg_3(VO_4)_2$ after a reaction with CCl_2F_2 at 723 K are shown in Fig. 9. For the V_2O_3 sample, the diffraction patterns of the remaining V_2O_3 and the formed VF_3 were observed. Vanadium chloride was not observed, probably due to the fact that vanadium chloride and chloride oxide evaporated if they were formed. For the $Mg_3(VO_4)_2$ sample, MgF_2, the remaining $Mg_3(VO_4)_2$, and a trace amount of $Mg_2V_2O_7$ as an impurity were observed after the reaction. $Mg_2V_2O_7$, which is observed as an impurity before the reaction, is considered to be left in the sample due to its low reactivity and/or structural changes of $Mg_3(VO_4)_2$ to $Mg_2V_2O_7$. Based on the results of a reactivity test showing that CO_2 was a major gaseous product, the reaction should proceed following;

$$Mg_3(VO_4)_2(s) + 3CCl_2F_2(g) \rightarrow 3MgF_2(s) + 3CO_2(g) + 2VOCl_3(g). \quad (5)$$

The results obtained for VM-He samples at high vanadium loading (Table 1) accompanying CO formation were similar to that for V_2O_3 (Table 4). Although no evidence on the presence of vanadium oxide on VM-He samples was acquired by the characterization, reduced vanadium oxides can exist on/in a VM-He sample. On the other hand, the results obtained for VM-air samples, which showed high CO_2 selectivity and no CO formation (Table 1), resembled those for $Mg_3(VO_4)_2$ (Table 4) with the results of the characterization. Needless to say, V_2O_3 and $Mg_3(VO_4)_2$, themselves, are not suitable for CCl_2F_2 decomposition and halogen fixation, since unstable halogenated and oxyhalogenated vanadium compounds formed tend to evaporate instead of fixing halogen in the solid phase. From this point of view, alkaline earth metal halides must be formed as the final solid-phase product.

Reaction of Vanadium Trihalide Oxide with Magnesium Oxide. Plausible aspects of the reaction between CCl_2F_2 and MgO and the effects of supported vanadium oxides on CCl_2F_2 decomposition were briefly described in our previous report,[7] i.e. vanadium oxide on MgO first reacts with CCl_2F_2 to form unstable vanadium halides or halide oxides, which sequentially react with MgO to regenerate vanadium oxide and to form magnesium halides. A yellowish deposition was also observed at the upper side of the reactor, similar to the case of $Mg_3(VO_4)_2$ during the decomposition by VM-air samples. At the exit (downstream) of the reaction zone, a dark-green deposition was observed. The XRD pattern of the deposit was assigned to be VOCl, which would be formed from $VOCl_3$ or $VOCl_2$. It has been reported that the disproportionation of $VOCl_2$ occurs, following equation by heating $VOCl_2$ in an inert atmosphere above 573 K or 603 K:[27]

$$2VOCl_2(s) \rightarrow VOCl(s) + VOCl_3(g). \quad (6)$$

There are many kinds of other vanadium halides, vanadium halide oxides, which are candidate for the reaction intermediate; some of them should play an important role in a halogen–oxygen exchange between CCl_2F_2 and MgO. Thus, we focused on two vanadium trihalide oxides, $VOCl_3$ and VOF_3. Assuming that these two compounds are formed as a reaction intermediate in CCl_2F_2 decomposition by VM-air samples, which have $Mg_3(VO_4)_2$ as an active phase; the reaction equation for the primary conversion of CCl_2F_2 can be described as follows in addition to Eq. 5:

$$3CCl_2F_2(g) + 2Mg_3(VO_4)_2(s) \rightarrow 2VOF_3(s) + 2VOCl_3(g) + 6MgO(s) + 3CO_2(g). \quad (7)$$

Since both VOF_3 and $VOCl_3$ are commercially available, VOF_3 and $VOCl_3$ were subjected to a reaction with MgO by physically mixing (V/MgO: 30 wt %) in a quartz reactor under stream of helium at 723 K for 3 h to confirm the reactivity of these vanadium halide oxides with MgO. After the quasi solid-phase reaction, XRD and FT-IR analyses were carried out to identify the products. The XRD patterns of the mixture after the reaction are shown in Fig. 10. It is clear that the thermal

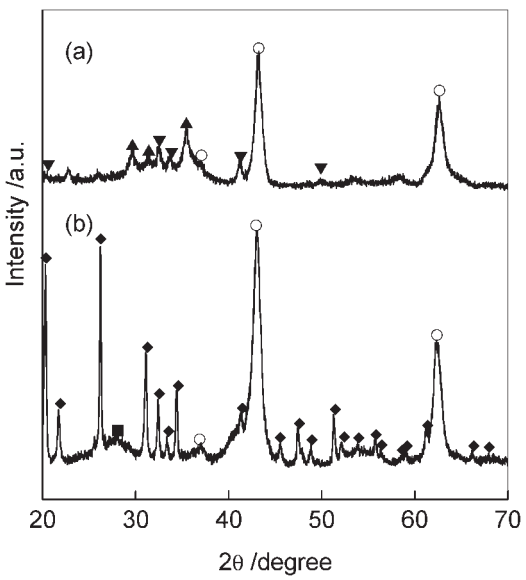

Fig. 10. XRD patterns of physically mixed sample composed of MgO and $VOCl_3$ (a) or VOF_3 (b) after thermal treatment at 723 K for 3 h. MgO (○), $Mg_3(VO_4)_2$ (▲), $MgCl_2 \cdot 6H_2O$ (▼), MgF_2 (■), and V_2O_5 (◆).

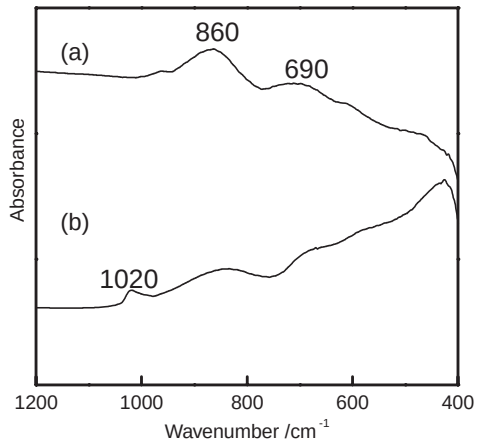

Fig. 11. FT-IR spectra of $VOCl_3$ (a) or VOF_3 (b) physically mixed with MgO treated at 723 K for 3 h.

solid-phase reaction of $VOCl_3$ with MgO resulted in the formation of $Mg_3(VO_4)_2$ as vanadium oxides and $MgCl_2$ as a final product of chlorine fixation. Although the vanadium oxide formed was not $Mg_3(VO_4)_2$, but V_2O_5, by a thermal reaction of VOF_3 with MgO, MgF_2 could be observed as the final product of fluorine fixation.

FT-IR spectra of the mixtures are shown in Fig. 11. For the mixture after the reaction of $VOCl_3$ with MgO, two distinct peaks were observed at 860 cm^{-1} and 690 cm^{-1}, which clearly indicate $Mg_3(VO_4)_2$ formation. However, V_2O_5 formation was observed only for that of VOF_3 with MgO. These results agreed with the XRD analysis. From these results it is concluded that $VOCl_3$ plays an important role in chlorine fixation during CCl_2F_2 decomposition by VM-air samples, since $Mg_3(VO_4)_2$, an active phase for CCl_2F_2 decomposition, can be regenerated and chlorine of $VOCl_3$ has been proven to be fixed as $MgCl_2$ in the presence of MgO, i.e. by the reaction between $VOCl_3$ and MgO described as follows:

$$2VOCl_3(g) + 6MgO(s) \rightarrow Mg_3(VO_4)_2(s) + 3MgCl_2(s). \quad (8)$$

Thus, $Mg_3(VO_4)_2$ can work catalytically through the change into/from $VOCl_3$ as CCl_2F_2 decomposition proceeds. On the other hand, since V_2O_5 is much less reactive than $Mg_3(VO_4)_2$ for CCl_2F_2 decomposition, VM-air samples would become less reactive if VOF_3 would be significantly produced by the reaction.

CCl_4 Decomposition by $Mg_3(VO_4)_2$ and V_2O_5. In our previous reports, we claimed that the reactivity to CCl_4 is important, since CCl_4 is a reaction intermediate as well as a by-product in CCl_2F_2 decomposition, and concluded that the highest halogen fixation ability of vanadium oxide among transition metal oxides on MgO is due to its high reactivity to CCl_4.[7] Actually, Klabunde et al. reported that vanadium oxide supported on MgO exhibits high reactivity to CCl_4, being consistent with our result.[2] As mentioned above, $Mg_3(VO_4)_2$ is found to be the active phase for CCl_2F_2 decomposition, and both $Mg_3(VO_4)_2$ and V_2O_5 can be catalytically regenerated from vanadium trihalide oxides; thus, the reactivity of both $Mg_3(VO_4)_2$ and V_2O_5 to CCl_4 is also crucial for the total decomposition of CCl_2F_2 to CO_2 and solid halides. Hence, we confirmed the reactivity to CCl_4 using a pulse-reaction system

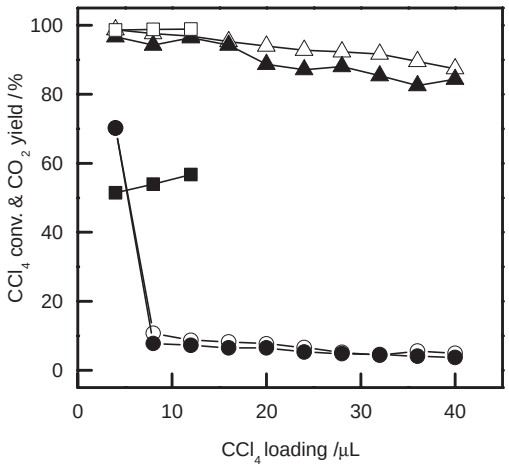

Fig. 12. CCl_4 decomposition by MgO (circle), V_2O_5 (square), and $Mg_3(VO_4)_2$ (triangle) using pulse reaction system. CCl_4 conversion (open), CO_2 yield (closed). Reaction temperature: 723 K, CCl_4 injection: 4 μL per pulse, the amount of sample: 0.2 g.

at 723 K. The results are shown in Fig. 12, including the result for MgO without the vanadium species (○ and ● for CCl_2F_2 conversion and CO_2 yield, respectively), which is quickly deactivated. While both $Mg_3(VO_4)_2$ and V_2O_5 exhibited a high conversion of CCl_4 (△ and □, respectively), the CO_2 selectivity was just 50% for V_2O_5. The reaction of V_2O_5 with CCl_4 is known to be a useful way to produce $VOCl_3$.[28,29] In this experiment another unknown peak was also observed in the products by GC-TCD analysis. The unknown product should be $COCl_2$, which is known to be the intermediate during CCl_4 decomposition; however, due to a lack of available authentic $COCl_2$, we were not able to identify the product. Taking these results into account, the reaction between V_2O_5 and CCl_4 can be described as follows:

$$V_2O_5(s) + 2CCl_4(g) \rightarrow 2VOCl_3(g) + CO_2(g) + COCl_2(g). \quad (9)$$

Since the reaction effluent was directly connected to the analysis column and the initial column temperature was as low as 333 K in GC-TCD analysis, a dark-green substance was observed at the inlet of the column packed with Porapak Q. In order to avoid spoiling the column packing, the reaction was terminated after 3 pulses of CCl_4 injection. The dark-green substance should be $VOCl_2$, which is known as an intermediate of $VOCl_3$ formation in the course of CCl_4 decomposition by V_2O_5.[28]

While both CCl_4 conversion (△) and CO_2 yield (▲) were very high in CCl_4 decomposition by $Mg_3(VO_4)_2$, the dark-green substance was also observed down stream of the reactor, i.e. the inlet in the column of GC-TCD. Assuming that the substance is the same as in the case for V_2O_5, the reaction of CCl_4 with $Mg_3(VO_4)_2$ can be described by the following equation:

$$3CCl_4(g) + Mg_3(VO_4)_2(s) \rightarrow 3CO_2(g) + 3MgCl_2(s) + 2VOCl_3(g). \quad (10)$$

This reaction also gives $VOCl_3$ as a product; however, as shown in Eq. 8, $VOCl_3$ can react with MgO to regenerate

$Mg_3(VO_4)_2$. 5VM-air sample was also highly reactive to CCl_4, decomposing almost 100% of at least 20 pulses of CCl_4, though the data are not shown in the figure. From these results, the high reactivity of VM-air samples to CCl_4 can be explained as follows: $Mg_3(VO_4)_2$ on/in VM-air samples reacts with CCl_4 to form $VOCl_3$, immediately followed by the sequential reaction of $VOCl_3$ with MgO to regenerate $Mg_3(VO_4)_2$, which is subjected to the reaction with CCl_4 again. In this way, VM-air samples can decompose CCl_4 catalytically.

Proposed Reaction Scheme for CCl_2F_2 Decomposition by VM-air Sample. Calcination of vanadium acetylacetonate on MgO in air gave $Mg_3(VO_4)_2$, which was also suggested to be the active species for CCl_2F_2 decomposition. The following reaction scheme was proposed from the above results. $Mg_3(VO_4)_2$ has Lewis acidity and CCl_2F_2 decomposition is initiated by the Lewis-acid sites to dissociate C–F bonding of CCl_2F_2. Major products are MgF_2 and CO_2 (Eq. 5). $VOCl_3$ and a small amount of VOF_3 are also formed as intermediates. $VOCl_3$ and VOF_3 are unstable and react with MgO to form vanadium oxides (as $Mg_3(VO_4)_2$ and V_2O_5, respectively), $MgCl_2$, and MgF_2. The above reaction scheme is shown in Fig. 13a as a main (initial) reaction pathway. In this figure, the formation of VOF_3 was omitted due to the minor contribution.

During the decomposition, CCl_4 is formed through two pathways: conversion of CCl_2F_2 (Eq. 2) at the Lewis-acid site generated by the fluorination of MgO and the halogen exchange reaction between $MgCl_2$ and CCl_2F_2 (Eq. 3). CCl_4 is not substantially decomposed by MgO, but effectively decomposed by $Mg_3(VO_4)_2$ or V_2O_5 accompanying the formation of $VOCl_3$ and CO_2 (Fig. 12). Formed $VOCl_3$ reacts with MgO, forming $Mg_3(VO_4)_2$. In this way, CCl_2F_2 decomposition proceeds catalytically, mainly by $Mg_3(VO_4)_2$ through the change between $VOCl_3$ and $Mg_3(VO_4)_2$. The scheme of this side reaction is shown in Fig. 13b.

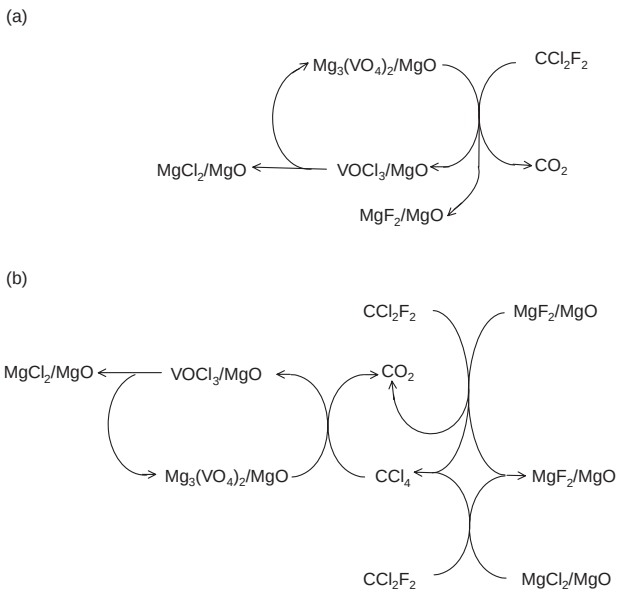

Fig. 13. The reaction scheme of CCl_2F_2 decomposition by VM-air sample. (a) Main (initial) reaction pathway, (b) side reaction pathway.

This reaction is appreciably affected by the loading of vanadium. When vanadium loading was as low as 1 wt %, the induction period was observed as shown in Fig. 1. This is due to a lack of acidity to trigger CCl_2F_2 conversion. Although the initial conversion of CCl_2F_2 is low, it increases to 100% after the induction period, during which the acidity increases by the fluorination of MgO. These partially fluorinated MgO sites can decompose CCl_2F_2 to CCl_4, CO_2, and MgF_2, as described in our previous report.[8] During this process, CO_2 selectivity should be almost 50%; however, CO_2 selectivity is actually as high as 90%, as shown in Table 1, indicating that the formed CCl_4 was significantly decomposed by the $Mg_3(VO_4)_2$. Thus, in the case of low vanadium loading, which does not have sufficient acid sites, CCl_2F_2 is decomposed mainly by the partially fluorinated MgO sites. We consider that vanadium oxide acts as an initiator of CCl_2F_2 decomposition to form partially fluorinated MgO sites in the first stage, and also acts as a catalyst to decompose CCl_4 and to promote fixation of chlorine all the way.

As shown in Table 2, the acidity of MgO increases as vanadium loading increases to 5 or 10 wt %. 5 wt % vanadium oxide supported on MgO, which has sufficient acid sites, gives either a high initial conversion of CCl_2F_2 and a high CO_2 selectivity. In this case, $Mg_3(VO_4)_2$ promotes the conversion of both CCl_2F_2 and an intermediate, CCl_4. Although high CO_2 selectivity is attained at the beginning, this gradually decreases accompanying CCl_4 formation. CCl_4 is formed mainly by the reaction of $MgCl_2$ with CCl_2F_2. In this way, vanadium loading is important to increase both CCl_2F_2 conversion and CO_2 selectivity; the latter is related to the ability of CCl_4 decomposition.

On the other hand, when the CO_2 yield is plotted against MgO conversion, it decreases with the amount of MgO left, as shown in Fig. 2. From this aspect, the exchange reaction between bulk halogen and oxygen is also important.

Generally speaking, which is called destructive absorption (or adsorption) consists of two parts: gas–solid reaction and surface regeneration with an exchange reaction between halogen and oxygen (migration of halogen); the latter reaction contains the bulk reaction, too. As described in our previous paper, the fixation rate of fluorine by MgO is much faster than that of chlorine,[8] which causes the MgO surface to be temporarily covered by chlorine. The covered chlorine is removed by halogen-exchange reaction with CCl_2F_2, and converted to MgF_2 and CCl_4 (Eq. 3), as is shown in this study. This behavior would be basically derived from the character of MgO. On the other hand, chlorine was effectively absorbed in the presence of vanadium oxide; $Mg_3(VO_4)_2$ promotes CCl_4 decomposition and chlorine fixation to the bulk. In this case, $Mg_3(VO_4)_2$ promotes not only the surface reaction, but also the bulk reaction to fix chlorine, although the details of this mechanism are not clearly understood at present.

As shown in Fig. 3, the decomposition of CCl_4 becomes difficult and the halogen-exchange reaction (Eq. 3) becomes the main reaction when MgO is consumed. Intermediate $VOCl_3$ was found to evaporate from the surface, and VOF_3 or V_2O_5 was also deposited at the inner side of the reactor when MgO was sufficiently consumed. Although the exact amount of evaporated vanadium could not be estimated. Even at this

stage, CCl_2F_2 is still converted (but the reaction path is changed), since sufficient $MgCl_2$ is left to undergo the halogen exchange reaction (at the final stage of the reaction). The halogen exchange is not a catalytic reaction, and continues until the conversion of $MgCl_2$ to MgF_2 is completed.

Conclusion

CCl_2F_2 decomposition with halogen fixation by vanadium oxide supported on magnesium oxide was studied by using vanadium acetylacetonate as a precursor of vanadium oxide supported on MgO. When the precursor sample was heated in air, $Mg_3(VO_4)_2$ was formed, which was confirmed by all of XRD, FT-IR, Raman, and XPS, while it was not observed when the sample was treated under helium. $Mg_3(VO_4)_2$ was revealed to be an active phase for CCl_2F_2 decomposition with complete halogen fixation as MgF_2 and $MgCl_2$. The details of the reaction mechanism are as follows: CCl_2F_2 decomposition is initiated by Lewis-acid site on $Mg_3(VO_4)_2$ to dissociate C–F bonding accompanying fluorine fixation as MgF_2. The intermediate product $VOCl_3$ reacts with MgO to regenerate the active $Mg_3(VO_4)_2$ phase with chlorine fixation as $MgCl_2$. Intermediate CCl_4 can also be decomposed by $Mg_3(VO_4)_2$ to form $VOCl_3$. The turnover between $Mg_3(VO_4)_2$ and $VOCl_3$ is considered to bring the high activity of CCl_2F_2 decomposition by vanadium oxide supported on MgO.

Experimental

Materials. MgO (UBE Materials Industries, 100A) was suspended to highly purified water and heated to be dried up; then, the resulting $Mg(OH)_2$ was treated at 873 K for 3 h under helium. MgO obtained by this method has a specific surface area of 170–210 $m^2\,g^{-1}$. Vanadium acetylacetonate complex ($V(acac)_3$, Aldrich) was dissolved into tetrahydrofuran (THF) and the MgO was added to the solution. Then, THF was removed from the resulting suspension with a rotary evaporator and the residue was dried in an oven at 373 K. Ligand removal from vanadium acetylacetonate was carried out at 873 K for 3 h under air or helium. The sample was denoted as 5VM-air when the sample had vanadium loading of 5 wt % (V/MgO = 0.05) and was calcined under air.

V_2O_3, V_2O_4, and V_2O_5 were obtained from commercial sources (Aldrich). Three kinds of magnesium vanadates ($Mg_3(VO_4)_2$, $Mg_2V_2O_7$, and MgV_2O_6) were prepared by the following method.[14] After $Mg(NO_3)_2\cdot 6H_2O$ (Wako Pure Chem. Ind.) and NH_4VO_3 (Kanto Kagaku) were dissolved into highly purified water, citric acid (Wako Pure Chem. Ind.) was added to the solution. The mole amount of added citric acid was the same as those of Mg and V. The solution was concentrated under reduced pressure to be dried up. The resulting precursor was heated at 573 K for 16 h and 873 K for 20 h under air. All of the magnesium vanadates were identified by XRD (Rigaku Multiflex S, Cu Kα).

CCl_2F_2 Decomposition. Reactions of CCl_2F_2 with vanadium oxides supported on MgO, authentic vanadium oxides, and magnesium vanadates were performed using a fixed-bed flow reactor system at atmospheric pressure. 1% CCl_2F_2 balanced with helium was fed to 0.2 g of a sample placed in a tubular quartz reactor at 723 K with a total flow rate of 30 mL min^{-1} after the sample was pretreated under helium flow at 873 K for 3 h. An analysis of the outlet gas was carried out using a GC-TCD (Shimadzu GC-14B) with a Porapak Q column to determine the conversion of CCl_2F_2 and the selectivity to carbon dioxide. 3.3 h feeding of CCl_2F_2 corresponds to the stoichiometry (CCl_2F_2/MgO = 0.5 mol mol^{-1}). If complete decomposition of CCl_2F_2 into CO_2 and magnesium halides is achieved following Eq. 1, MgO is totally turned to $MgCl_2$ and MgF_2 at this period of time. The conversion of MgO was estimated by the amount of formed CO_2, since the oxygen source in the system was only the lattice oxygen in MgO with a small amount of vanadium oxides. For the VM sample MgO conversion was calculated ignoring the amount of vanadium added to MgO.

CCl_4 Decomposition. CCl_4 decomposition by MgO, V_2O_5, and $Mg_3(VO_4)_2$ was carried out using a fixed-bed pulse reaction system directly connected to GC-TCD. Pulses of 4 μL of CCl_4 (Wako Pure Chem. Ind., 99%) in a precision syringe were injected to the same reactor as CCl_2F_2 decomposition at 723 K.

Characterization. X-ray diffraction patterns of the samples were obtained with Rigaku Multiflex S with Cu Kα as an incident X-ray source in the range of 20 to 70 degrees as 2θ. A specific surface area of the samples was determined by nitrogen adsorption at 77 K with BELSORP 28SA (BEL Japan). Infrared spectra were obtained with a JASCO FT-IR 350. The sample was diluted with KBr and pressed into a thin wafer. Raman spectra were taken with a JASCO RMP-200 at ambient atmosphere. The XPS analysis was performed by the ULVAC-PHI 1700R ESCA system with a monochromated Al X-ray source. NH_3-TPD (temperature programmed desorption of ammonia) experiments were carried out for MgO samples by using a Pyrex-glass system equipped with a quartz U-tube reactor. The samples were pretreated at 873 K for 2 h under evacuation. After the sample was cooled down to 373 K, gaseous ammonia was introduced to the system, and then adsorption equilibrium was attained within 0.5 h. NH_3-TPD was performed at a temperature ramping rate of 10 K min^{-1} from 373 K to 873 K with detection by TCD (Shimadzu GC-8A) after removing physisorbed ammonia under a vacuum for 0.5 h.

References

1 K. J. Klabunde, J. Stark, O. Koper, C. Mohs, D. G. Park, S. Decker, Y. Jiang, I. Lagadic, and D. Zhang, *J. Phys. Chem.*, **100**, 12142 (1996).

2 Y. Jiang, S. Decker, C. Mohs, and K. J. Klabunde, *J. Catal.*, **180**, 24 (1998).

3 K. J. Klabunde, A. Khaleel, and D. Park, *High Temp. Mater. Sci.*, **33**, 99 (1995).

4 S. P. Decker, J. S. Klabunde, A. Khaleel, and K. J. Klabunde, *Environ. Sci. Technol.*, **36**, 762 (2002).

5 O. Koper, I. Lagadic, and K. J. Klabunde, *Chem. Mater.*, **9**, 838 (1997).

6 O. Koper, E. A. Wovchko, J. A. Glass, J. T. Yates, and K. J. Klabunde, *Langmuir*, **11**, 2054 (1995).

7 T. Tamai, K. Inazu, and K. Aika, *Chem. Lett.*, **32**, 436 (2003).

8 T. Tamai, K. Inazu, and K. Aika, *Bull. Chem. Soc. Jpn.*, **77**, 1239 (2004).

9 E. Kemnitz, A. Hess, G. Rother, and S. Troyanov, *J. Catal.*, **159**, 332 (1996).

10 A. Alonso, A. Morato, F. Medina, Y. Cesteros, P. Salagre, and J. E. Sueiras, *Appl. Catal., B*, **40**, 259 (2003).

11 H. H. Kung and M. C. Kung, *Appl. Catal., A*, **157**, 105 (1997).

12 T. Blasco, J. M. López Nieto, A. Dejoz, and M. I. Vázquez, *J. Catal.*, **157**, 271 (1995).

13 D. S. H. Sam, V. Soenen, and J. C. Volta, *J. Catal.*, **123**, 417 (1990).

14 X. Gao, P. Ruiz, Q. Xin, X. Guo, and B. Delmon, *J. Catal.*, **148**, 56 (1994).
15 M. A. Chaar, D. Patel, M. C. Kung, and H. H. Kung, *J. Catal.*, **105**, 483 (1987).
16 D. Patel, P. J. Andersen, and H. H. Kung, *J. Catal.*, **125**, 132 (1990).
17 X. Gao, P. Ruiz, Q. Xin, X. Guo, and B. Delmon, *Catal. Lett.*, **23**, 337 (1994).
18 J. M. López Nieto, A. Dejoz, M. I. Vázquez, W. O'Leary, and J. Cunningham, *Catal. Today*, **40**, 215 (1998).
19 A. Corma, J. M. López Nieto, and N. Paredes, *J. Catal.*, **144**, 425 (1993).
20 G. A. M. Hussein, *Thermochim. Acta*, **256**, 347 (1995).
21 N. Krishnamachari and C. Calvo, *Can. J. Chem.*, **49**, 1629 (1971).
22 G. Martra, F. Arena, S. Coluccia, F. Frusteri, and A. Parmariana, *Catal. Today*, **63**, 197 (2000).
23 A. Pantazidis, A. Auroux, J.-M. Herrmann, and C. Mirodatos, *Catal. Today*, **32**, 81 (1996).
24 H. Noller, J. A. Lercher, and H. Vinex, *Mater. Chem. Phys.*, **18**, 577 (1998).
25 F. A. Miller and L. R. Cousins, *J. Chem. Phys.*, **26**, 329 (1957).
26 R. J. H. Clark, "The Chemistry of Vanadium," Pergamon Press, Oxford (1975).
27 A. Yajima, R. Matsuzaki, and Y. Saeki, *Bull. Chem. Soc. Jpn.*, **53**, 35 (1979).
28 S. B. Geyer, L. R. Brock, J. W. Keister, and T. C. Devore, *Proc. Electrochem. Soc.*, **97**, 298 (1997).
29 G. Mink, I. Bertoti, I. S. Pap, T. Szekely, C. Battistoni, and E. Karmazsin, *Thermochim. Acta*, **85**, 83 (1985).